Exciton Diffusion Length and Lifetime in Subphthalocyanine Films

ARTICLE *in* THE JOURNAL OF PHYSICAL CHEMISTRY C · FEBRUARY 2009

Impact Factor: 4.77 · DOI: 10.1021/jp809802q

Exciton Diffusion Length and Lifetime in Subphthalocyanine Films

H. Gommans, S. Schols,*,†,‡ A. Kadashchuk, and P. Heremans†

IMEC v.z.w., SOLO/PME, Kapeldreef 75, 3000 Leuven, Belgium

S. C. J. Meskers

Molecular Materials and Nanosystems, Eindhoven University of Technology, Eindhoven, The Netherlands

Received: November 6, 2008; Revised Manuscript Received: December 16, 2008

Organic photovoltaic cells with chloro[subphthalocyaninato]boron(III) (SubPc) as donor in combination with buckminster fullerene (C_{60}) as acceptor in a planar heterojunction configuration have shown high power conversion efficiencies. The parameter that determines the critical distance to the heterojunction over which light-generated excitons can be harvested is the exciton diffusion length. Here, we characterize this exciton diffusion length in SubPc thin films by photoluminescence (PL) quenching experiments in a planar bilayer system. As the layer thickness is much smaller than the optical penetration depth, we apply the transfer matrix method (TMM) to calculate the internal optical field inside the organic structures and use this to derive the intrinsic PL spectrum. An exciton diffusion length of 28 nm is determined, and good agreement is found with the diffusion lengths obtained from modeling the external quantum efficiency. In addition, time-resolved PL measurements are performed to determine the exciton lifetime to be 0.3 ns.

1. Introduction

In organic semiconductors, the dissociation efficiency of excitons into free carriers is small (≤ 0.01) because of the strong competing process of geminate pair recombination. According to the Onsager theory,[1] the latter is a result of the low relative dielectric constant in organic materials (~ 3). Heterojunctions between donor and acceptor materials with proper energy offset solve this problem,[2] as charge transfer at the interface results in the formation of a metastable geminate electron−hole pair, thereby increasing the conversion rates. However, only excitons generated near the heterojunction can benefit from this enhanced dissociation. The parameter that characterizes the average distance over which an exciton can diffuse between its generation and its recombination is the exciton diffusion length L_D. Therefore, the exciton diffusion length is a critical parameter in the conversion efficiency for organic heterojunction solar cells. Recently, Terao et al.[3] characterized a nearly linear relationship between the short circuit current I_{SC} and L_D based on a set of six different metal-phthalocyanines (MPcs).

The accepted technique to determine the exciton diffusion length is photoluminescence (PL) quenching in a planar bilayer system. Here, the reduction in PL due to the presence of a quencher material at the surface is measured as a function of the layer thickness of the luminescent material.[4−8] In the past, alternative methods have been used such as sensitized fluorescence, whereby a luminescent guest was mixed in an absorbing host material. However, debate over its interpretation spurred off, as the spread in diffusion constant in similar materials appeared to be as large as 2−3 orders of magnitude.[9] This spread was attributed to the impossibility to characterize capture and diffusion rates independently.

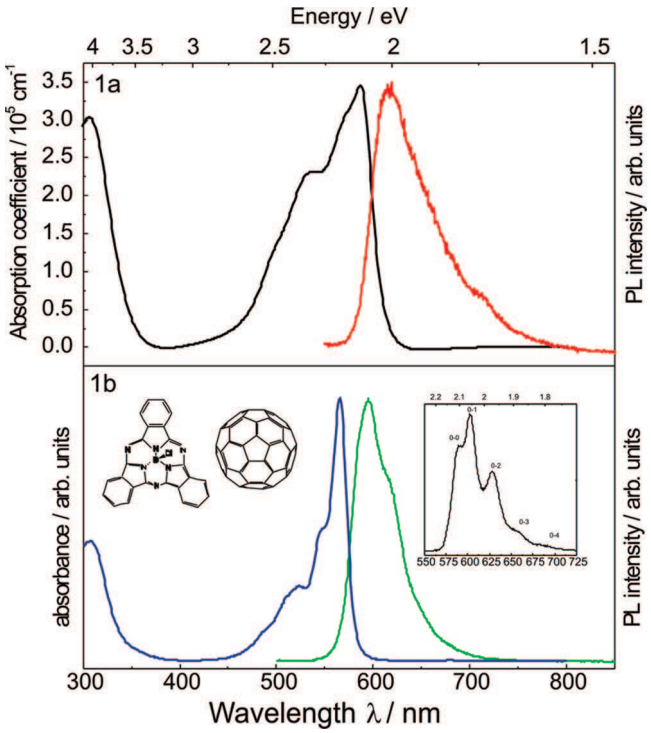

Figure 1. (a) SubPc absorption coefficient (black) as determined from ellipsometry and the PL spectrum (red) of 10 nm SubPc deposited on a quartz substrate. (b) Absorbance (blue curve) and PL spectrum (green curve) of SubPc in a 2×10^{-3} wt % toluene solution at room temperature. Inset: PL spectrum of the frozen SubPc toluene solution at 80 K; structural formulas of SubPc and C_{60}.

Recently, it has been shown that chloro[subphthalocyaninato]boron(III) (SubPc) is a prospective material for organic photovoltaics.[10,11] The molecular formula is shown in Figure 1b: the molecule is composed of three diiminoisoindole rings N-fused around a boron core. The 14 π-electron aromatic

* Corresponding author. E-mail: sarah.schols@imec.be.
† Also at: Electrical Engineering Department, Katholieke Universiteit Leuven, B-3001 Leuven, Belgium.
‡ Aspirant at the FWO Vlaanderen.

10.1021/jp809802q CCC: $40.75
Published on Web 01/26/2009

macrocycle has a nonplanar cone-shaped structure, with the tetrahedral boron center out of plane with the aromatic ligand. Spectroscopic ellipsometry on vacuum-deposited SubPc films shows that, as compared to films of other well-known MPcs,[11] films of SubPc possess a high extinction coefficient of 1.6, and dielectric constant of 3.9. More details concerning its chemical properties can be found elsewhere.[12] Efficient photoinduced electron transfer in SubPc−C_{60} dyads has been demonstrated,[13] and a SubPc/C_{60} bilayer structure indeed gives rise to high photovoltaic power conversion efficiencies of 3% with a noteworthy high open-circuit bias.[11,14]

In the present Article, we report on the PL study of the exciton diffusion length in vacuum-deposited SubPc films. To derive the exciton diffusion length, the optical excitation profile in the emissive layer is calculated as a function of position. For this, we use software modeling based on TMM formalism that takes into account optical interference due to multiple interfaces in the structure, the angle of incidence and detection, the polarization angle, and photon reabsorption (trivial or radiative energy transfer). The effect of such phenomena on the interpretation of PL quenching has been previously established.[6,15] Time-resolved PL measurements have also been performed to determine the singlet exciton lifetime.

2. Experimental Section

SubPc and C_{60} were purchased from Aldrich and purified once by train sublimation before they were loaded into an ultrahigh vacuum system (base pressure 10^{-9} torr). Organic thin films were grown on precleaned quartz substrates (Corning Inc.) using organic molecular beam deposition. The rate (0.5−1.0 Å/s) was measured by a quartz crystal monitor that in turn was calibrated from determination of the layer thickness by spectroscopic ellipsometry (Sopra GESP-5). During deposition, the substrates were kept at room temperature. The film morphology was imaged ex-situ by atomic force microscopy (VEECO Dimension 3000) using an RTESPA tip operating in tapping mode.

PL measurements of the diluted solutions and films were carried out within a temperature range between 80 and 300 K, using a temperature-regulating N_2 cryostat. These measurements were done in N_2 atmosphere to prevent photo-oxidation. A N_2 laser with pulse duration of 4 ns operated at 10 Hz was used for optical excitation at 337 nm. The emission spectra were recorded using a triple-grating monochromator coupled to an intensified CCD camera (PI-MAX from Princeton Instruments), which was synchronized by the electrical trigger of the laser. To increase the signal-to-noise ratio, spectra were accumulated by averaging over 300 pulses. Absorption spectra were recorded using a Shimadzu UV-1601PC UV−vis scanning spectrometer.

PL quenching experiments were performed at room temperature in planar geometry for various SubPc layer thicknesses. The samples were excited by s-polarized 337 nm light at 0° incidence with the surface normal through the quartz substrate. Light detection was performed at 45° angle in reflection using the same monochromator and intensified CCD camera as for standard PL measurements. SubPc and SubPc/C_{60} samples were fabricated in the same run and measured under the same conditions.

Time-resolved fluorescence experiments were carried out with a 400 nm excitation pulse obtained from a Picoquant LDH C400 laser, operating at a repetition rate of 0.48 MHz. The fluorescence light, collected in a backward scattering geometry, was dispersed by a 0.34 m double monochromator, allowing for a spectral resolution of 1 nm. Time-resolved emission spectra were recorded with the time-correlated single photon counting technique in reversed mode using a microchannel plate photomultiplier (Hamamatsu R3809u-51) and a time-to-amplitude converter. The width of the instrument response function amounts to 60 ps FWHM. Using a single channel analyzer (EG&G), fluorescence spectra can be recorded within a variable, narrow time window after the excitation pulse. When recording time-resolved emission spectra, the maximal count rate of photons was kept low ($\sim 10^3$ s^{-1}) to prevent distortion of the spectra due to pulse pile-up effects.

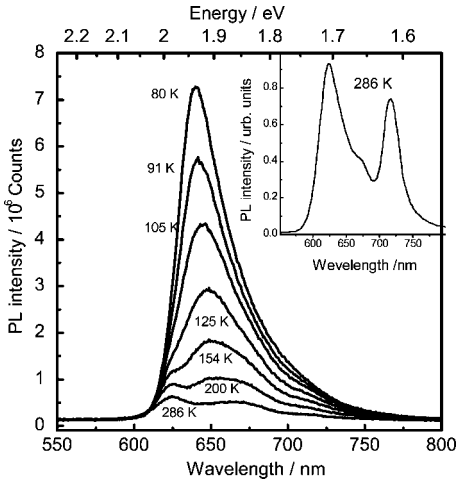

Figure 2. PL spectra recorded for a freshly prepared 100 nm SubPc film on a quartz substrate as a function of temperature. Excitation is performed at 337 nm unpolarized N_2 laser light at 45° incidence. Inset: Room-temperature PL spectrum of the film kept for a few days in a glovebox at room temperature.

3. Results and Discussion

3.1. General PL Characterization. Figure 1a presents the absorption and PL spectra of a 10 nm thick SubPc film on a quartz substrate at room temperature. The absorption coefficient of the film, α, was determined by spectroscopic ellipsometry. For PL measurements, excitation was performed using 337 nm N_2-laser light at 0° incidence angle with the surface normal. Figure 1b shows the room-temperature PL and absorption spectra of SubPc dissolved in a toluene ($c = 2 \times 10^{-3}$ wt %) solution. The PL spectrum of SubPc in a frozen toluene matrix at 80 K is depicted as the inset of Figure 1b. This spectrum clearly demonstrates a vibronic progression built on a 702 cm^{-1} mode, which together with the mirror symmetry in absorption and photoluminescence are generally explained by the Franck−Condon principle. The vibronic structure is not well resolved at room temperature, and the spectra are inhomogeneously broadened (Figure 1). The spectrum broadening is somewhat larger in SubPc film than in solution as expected for vapor deposited organic films, reflecting their polycrystalline/disordered structure. The apparent Stokes shift in the film is 890 cm^{-1}, resembling the 854 cm^{-1} obtained in solution.

The photoluminescence of a pristine 100 nm thick SubPc film on a quartz substrate as a function of temperature is shown in Figure 2. At room temperature, the 620, 670, and 710 nm peaks are clearly resolved. When decreasing the temperature to 80 K, the PL intensity increases with nearly an order of magnitude. In the temperature range between 80 and 150 K, the spectrum is rather unresolved. At temperatures exceeding 150 K, the emission redistributes and the 710 nm peak increases in intensity relative to the 670 nm emission. In freshly prepared samples, this 710 nm peak could be seen as a shoulder. The increase of PL intensity with decreasing temperature is a consequence of

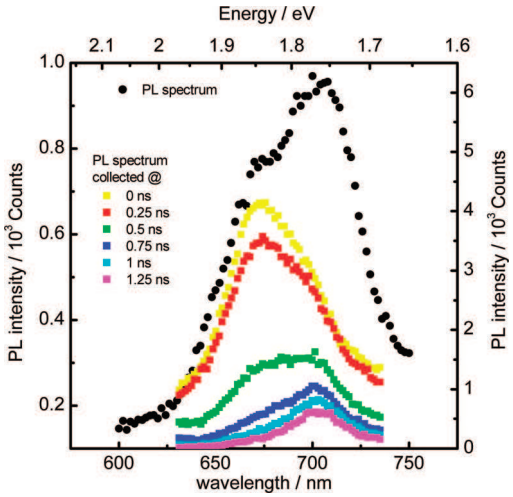

Figure 3. Time-resolved PL spectra of a 500 nm thick SubPc film on a quartz substrate. Excitation is performed at 400 nm.

decreased contributions from the nonradiative decay channels. In films, one expects an additional decay channel due to exciton diffusion toward bulk unidentified quenching centers. This may explain the emission redistribution with increasing temperature toward lower energies as well as the reduced exciton lifetime in films as compared to solution as discussed below. Both exciton diffusion as well as internal conversion are expected to decrease with decreasing temperatures.

Figure 3 shows the time-resolved PL spectra of a 500 nm thick SubPc film on a quartz substrate. Excitation is performed at 400 nm with linear polarized laser light at ~45° incidence with the surface normal, and the light detection is performed at a 45° angle. Although the absorption minimum between the Q-band and Soret (B) band is located near 400 nm, it was possible to generate and detect sufficient PL intensity. The evolution of the PL spectra with the delay time is obvious: the band peaking at 670 nm is the strongest in the PL spectrum at a delay time of ~0 ns, while the 710 nm band dominates the emission at a delay time of 1.25 ns (Figure 3), implying thus different decay rates for these spectral components. The time decay measured for the 670 and 710 nm PL bands is presented in Figure 4a and b, respectively. The lifetimes of these PL components are determined by fitting the measured time decay curves with (bi)exponential kinetics as shown in Figure 4. This yields lifetimes of 0.3 ns for the emission at 670 nm, and 0.4 and 2.15 ns at 710 nm band, which corresponds well to the observed singlet lifetimes of ~3 ns in benzene solutions.[16]

The results of time-resolved PL measurements suggest that the 710 nm peak has a different origin than the shorter-wavelength exciton component and it is most probably originated from some sort of structure defects in SubPc films. This is supported by the following observations: (i) we found that while the 710 nm peak is fairly weak in PL spectra in freshly prepared pristine SubPc films, its relative intensity notably increases after keeping the films for several days in a nitrogen glovebox at room temperature (inset to Figure 2). This effect may be explained by a gradual formation of structural defect states, due to aggregation at room temperature. (ii) The 710 nm PL peak is not seen in SubPc solution, suggesting that it is not related to molecular emission of SubPc. In addition, this low-energy PL peak was not observed in a SubPc solution after storing for days in ambient atmosphere; hence, oxidation can be excluded as its origin.

It should be mentioned that efficient generation of triplets in SubPc via intersystem crossing has been observed in argon-

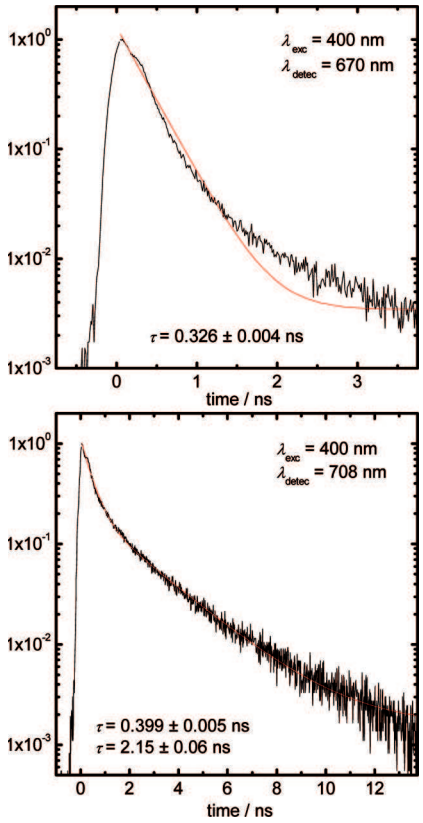

Figure 4. Time decay kinetics of 670 and 708 nm PL peaks of a SubPc film fitted with an exponential and biexponential decay function, respectively.

saturated SubPc solutions in benzene by photoinduced absorption measurements,[16] and a lifetime of 82 μs was found. The upper limit of the energy level of the lowest excited triplet state E_T of SubPc was indirectly estimated as 1.81 eV (690 nm).[16] However, we rule out phosphorescence as the origin of the 710 nm peak in these films because (i) in contrast to films, this peak was not detected in PL spectra of frozen diluted SubPc solution; and (ii) its temperature dependence in films is opposite from that expected for phosphorescence. In frozen diluted solution, triplet excitations are immobile and therefore are much less prone to nonradiative structure-induced quenching centers. Therefore, phosphorescence in diluted solutions is normally much stronger than in the solid state. For the same reason, triplet emission in films is expected to increase at low temperatures due to hampered diffusion toward the quenching centers. However, in our case, the opposite behavior is observed. In addition, the measured lifetime of 2.15 ns is too small for phosphorescence emission. Hence, we ascribe the low-energy PL peak at 710 nm to the emission of trapped excitation species at structural defects in SubPc film. This also explains the larger lifetime of this emission component as compared to the higher-energy peak at 670 nm (2.15 vs 0.32 ns), as expected for confined excitations.

The higher-energy PL emission band we ascribe to bulk excitons that can diffuse through the film and therefore show a shorter apparent lifetime as compared to that in diluted solution. Consequently, we will conduct the PL quenching analysis for this short-wavelength emission band.

3.2. PL Quenching Measurements. Figure 5a depicts the PL spectrum of the pristine SubPc layer as a function of thickness. The peak intensity for a 10 nm thick film is located near 615 nm and gradually shifts toward 638 nm for the 60 nm

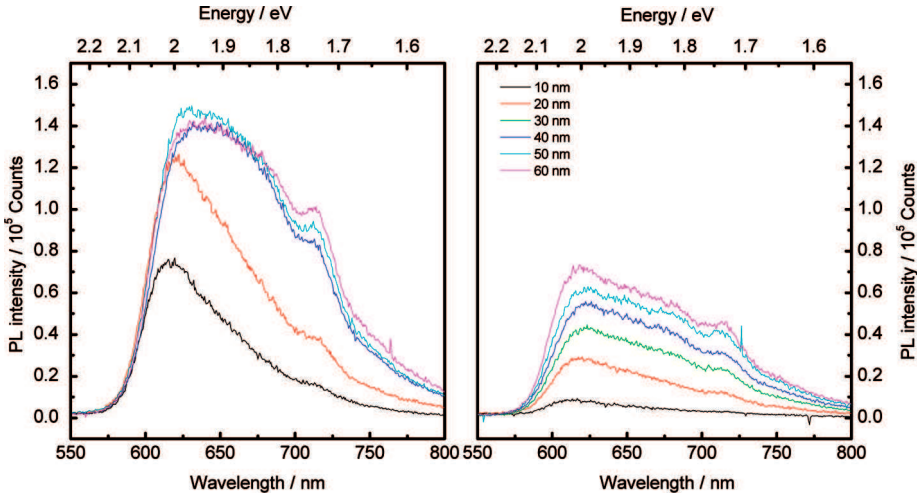

Figure 5. PL spectra recorded at room temperature as a function of SubPc layer thickness w/o C_{60} (a) and with C_{60} (b). Excitation is performed for an s-polarized 337 nm light wave at 0° incidence.

thick film. Additional peaks are located at 670 and 715 nm. An apparent trend in PL spectra with increasing film thickness is observed. For the moment, however, we refrain from straightforward interpretation, as in the final PL data analysis interference effects will be taken into account. Figure 5b demonstrates the PL spectrum of a quartz/SubPc/C_{60} structure measured under identical conditions. It can be immediately observed that the PL is reduced in intensity with respect to the structures without C_{60} layer and that the spectral shape is modified. This implies that different components of the PL spectra are quenched in unequal amounts: around 1.8−2.0 eV the PL intensity is more reduced as compared to the 1.75 eV peak. This behavior is quite expected as only mobile excitons can reach the quenching interface with C_{60}, while the 1.75 eV peak, ascribed before to localized excitation species, decreases in intensity due to C_{60}-induced reduction of the total bulk exciton concentration.

The most common procedure in PL quenching experiments comes down to determining the relative quenching efficiency, $Q(L)$, defined as $(Y_{NQ}-Y_Q)/Y_{NQ}$, as a function of the luminescent film thickness, L. Here, Y_{NQ} (Y_Q) is the PL yield in the absence (presence) of the quenching material. Considering that the coherence time τ_c at room temperature is much less than 10^{-13} s due to exciton−lattice interactions, the transport mechanism in the PL quenching experiments at time scales 10^{-9} s is understood to be a random hopping-like process, which is described by classical diffusion.[17] The continuum diffusion equation is:

$$\frac{\partial n(z,t)}{\partial t} = D\frac{\partial^2 n(z,t)}{\partial z^2} + g(z,t) - k_0 n(z,t) - F(z)n(z,t) \quad (1)$$

where D is the diffusion coefficient, $g(z, t)$ is the generation rate, $k_0 = 1/\tau_0$ is the decay rate constant, τ_0 is the exciton lifetime, and $F(z)$ is quenching rate profile. By imposing a constant value for the (partial derivative in z of the) exciton concentration, at either side of the luminescent film, two steady-state solutions are determined: one for the film with and one for the film without the quenching interface for arbitrary luminescent film thickness. In this manner, an analytical expression for $Q(L)$ is derived at which one can fit the experimental data points, with the exciton diffusion length, L_D, as a free parameter. The difficulty with this procedure in our case is 2-fold.

(i) The steady-state condition is generally not met for the fluorescence spectrum as the characterization time should allow for a homogeneous exciton concentration in the complete film. The time interval that we use to measure is determined by the singlet exciton lifetime and hence in the order of nanoseconds. The steady-state condition thus leads to a lower limit of the diffusion coefficient, which is already unrealistically large (10^4 nm^2/1 ns = 10^{-1} cm^2/s).

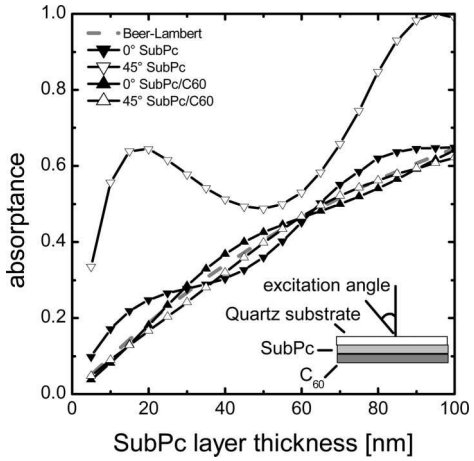

Figure 6. Calculated absorbance in SubPc as a function of layer thickness. Excitation is performed for an s-polarized 337 nm light wave at 0° and 45° incidence.

(ii) The absorption profile is often approximated with the Beer−Lambert law. This generation term then allows for analytical solutions for the diffusion equation. In our case, the film thickness is much smaller than the penetration depth, and hence explicit interference effects due to multiple refractive interfaces must be taken into account. This could lead to remarkable effects, as for instance the presence of the quenching layer already affects the absorption profile even if the light beam is first incident on the fluorescent material. A straightforward derivation of quenching ratios from the measured PL spectra as in Figure 5 is thus prone to error because the SubPc absorbance as well as the excitation profile is modified by the presence of C_{60}. This is illustrated in Figures 6 and 7, respectively. Figure 6 shows the absorbance for an S-polarized 337 nm excitation wavelength in SubPc as a function of SubPc layer thickness. The absorbance is calculated for incident angle of 0° and 45° and for the alternating presence and absence of a 30 nm C_{60} layer. For comparison, the Beer−Lambert (B−L) law is also shown as a function of layer thickness. The typical

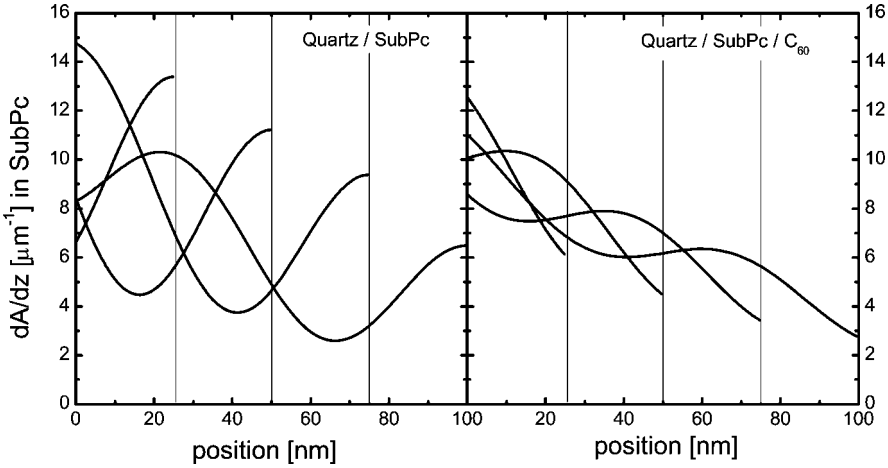

Figure 7. Calculated excitation profile in SubPc as a function of position in a quartz/SubPc (left) and quartz/SubPc/C_{60} (right) structure for 25, 50, 75, and 100 nm SubPc. Excitation is performed for an s-polarized 337 nm light wave at 0° incidence.

correction for such ultrathin films when allowing for interference due to multiple refractive interfaces is a sinusoidal function superimposed to the B−L law. For the 0° incidence, it can be observed that this sinusoidal obtains a phase shift when adding 30 nm of C_{60}. Hence, the absorption curves in the two structures, either including or excluding C_{60}, have multiple crossing points. In addition, a 30 nm C_{60} layer also modifies the excitation profile in the SubPc layer, as is demonstrated in Figure 7. The maxima in the excitation profile are typically shifted from the SubPc−air interface toward the middle of the film in case 30 nm C_{60} is included.

To correct for these effects, we will determine the intrinsic PL spectrum in SubPc, which is defined as the PL spectrum that is corrected for the geometric, interference, and self-absorption effects in the layered structure. This intrinsic PL will be used to estimate the PL yield for the structure with the additional 30 nm C_{60} layer in case it would not act as a quenching interface, Y_{NQ}. To derive the intrinsic PL, we assume a static exciton concentration in the SubPc film; that is, the emission profile equals the excitation profile in the emissive layer. Subsequently, $Q(L)$ is derived solely from the bilayer system using the calculated PL yield for Y_{NQ} and the measured PL yield (Figure 5b) for Y_Q.

To determine the intrinsic PL spectrum, three damped harmonic oscillators with resonance frequencies at 16 400, 14 800, and 13 900 cm^{-1} were fitted by their resonance strength and damping constants to the PL spectra in Figure 5a, accounting for the optical refractive indices of air, substrate, SubPc, and the angle of incidence, detection, and polarization. In this manner, the internal PL spectrum for each SubPc layer is derived and shown in Figure 8. The gradual change in line shape observed as a function of layer thickness (Figure 5a) has disappeared in the intrinsic PL spectrum (Figure 8). However, the absolute intensity of the intrinsic PL spectrum for SubPc samples appears not to be constant for the various thicknesses. Repetitive measurements yielded highly reproducible PL intensities that as a result did not lead to convergence of the calculated intrinsic PL spectrum. This indicates that surface, interface, and bulk relaxation effects in SubPc unintentionally play a role. To determine the quenching efficiency, we used one (mean) set of values, that of 20 nm SubPc, to calculate Y_{NQ}.

In Figure 9, two sets of quenching efficiencies, $Q^{ex}(L)$ and $Q(L)$, are shown as a function of layer thickness. Here, $Q^{ex}(L)$ is calculated by using the measured PL intensity at 624 nm

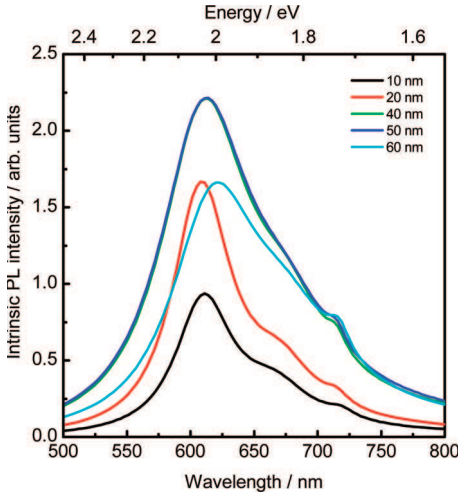

Figure 8. Intrinsic PL spectrum derived from quartz/SubPc structures with 10, 20, 40, 50, and 60 nm SubPc.

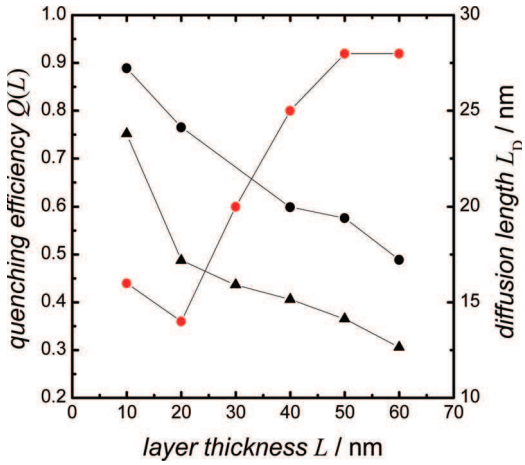

Figure 9. Left axis: Quenching efficiency in SubPc $Q^{ex}(L)$ (●) and $Q(L)$ (▲) vs SubPc layer thickness, L, at 624 nm in Figure 1. Right axis: Exciton diffusion length as determined from $Q(L)$ (red ●).

obtained on the structure without C_{60} (Figure 5a) for Y_{NQ}, while $Q(L)$ is derived using the calculated PL yield for Y_{NQ}. In the range from 10 to 60 nm, the quenching efficiency reduces from 0.9 to 0.5 for $Q^{ex}(L)$ and from 0.8 to 0.3 for $Q(L)$. To relate $Q(L)$ to a quenching distance (exciton diffusion length), the excitation profile is convoluted by a quenching probability determined by the distance to the SubPc−C_{60} interface. For such

quenching probability, a Bernoulli random walk in one dimension near an absorbing barrier is assumed. The probability, $P(x,\tau_0)$, that an exciton, initially ($t = 0$) at a distance x from the C_{60} interface, will be absorbed before it decays at $t = \tau_0$ equals $P(x,\tau_0) = 1 - \mathrm{erf}(x/\sqrt{4D\tau_0})$, where erf is the error function and D is the diffusion coefficient.[18] The exciton diffusion length in one dimension, L_D, is defined as $(2D\tau_0)^{1/2}$.[17]

Starting from the optical excitation profile, we derive a diffusion length for each layer thickness separately. These values are summarized in Figure 9. For the stochastic description to be valid, a large number of displacements are assumed. Moreover, the effect of the quartz/SubPc interface is neglected as we are ignorant of its reflecting or absorbing properties on the exciton dynamics. Hence, from the limited layer thickness range (10−60 nm), it can be argued that the estimated diffusion length becomes more accurate with increasing layer thickness. For SubPc layer thicknesses larger than 40 nm, we estimate L_D to be 28 nm. Note that the surface roughness of vacuum-deposited SubPc is proven small, root-mean-square equals 4.4 Å,[11] which is imperative in photoluminescence surface quenching as it determines the error for the diffusion length. The exciton diffusion length of 28 nm and a singlet lifetime of 0.3 ns yield a diffusion coefficient of 1×10^{-2} cm^2/s.

Another method to derive L_D is by modeling the measured external quantum efficiency, η_{EQE}, in organic photovoltaic cells (OPVC).[19] This is also performed by applying the TMM formalism in combination with the classical diffusion equation, and both techniques include thus similar physical processes. However, as η_{EQE} is based on detection of an electrical response, minimally two layers are added to the structure acting as electrodes. Generally, the exciton conversion efficiency as well as the charge collection efficiency are considered to be 1. These assumptions lead to an underestimation of L_D. The η_{EQE} of the OPVC, glass/indium−tin−oxide (ITO) (100 nm)/SubPc (13 nm)/C_{60} (32.5 nm)/bathocuproine (BCP) (10 nm)/Al (80 nm), has been measured and modeled in ref 20. There, L_D for SubPc was determined to be 13.4 nm, closely matching the measurement of Figure 9 for a film thickness of 10−20 nm. In addition, the L_D of SubPc in OPVC also seems comparable to the values of their planar MPcs counterparts that were observed to be in the range of 1.0−15.7 nm by modeling η_{EQE}'s.[3]

4. Conclusion

In summary, we have studied the photophysical properties in SubPc films. The internal optical field was calculated by modeling software based on TMM formalism. The intrinsic PL emission spectrum has been determined and included in the characterization for the diffusion length. Good agreement was found between diffusion lengths derived from PL quenching experiments and values obtained from modeling the external quantum efficiency. The exciton diffusion length converges toward 28 nm for a film thickness ≥40 nm, and the lifetime has been observed to be 0.3 ns. The long exciton diffusion length of SubPc and the high extinction coefficient of 1.6 make this material an attractive candidate as donor for heterojunction organic photovoltaic cells.

Acknowledgment. This work is supported by the EU-funded Project NAIMO (contract no. 500355). S.S. acknowledges the FWO Vlaanderen for financial support.

References and Notes

(1) Onsager, L. *Phys. Rev.* **1938**, *54*, 554.
(2) Tang, C. W. *Appl. Phys. Lett.* **1985**, *48*, 183.
(3) Terao, Y.; Sasabe, H.; Adachi, C. *Appl. Phys. Lett.* **2007**, *90*, 103505.
(4) Gregg, B. A.; Sprague, J.; Peterson, M. W. *J. Phys. Chem. B* **1997**, *101*, 5362.
(5) Haugeneder, A.; Neges, M.; Kallinger, C.; Spirkl, W.; Lemmer, U.; Feldmann, J.; Scherf, U.; Harth, E.; Gugel, A.; Mullen, K. *Phys. Rev. B* **1999**, *59*, 15346.
(6) Theander, M.; Yartsev, A.; Zigmantas, D.; Sundström, V.; Mammo, W.; Andersson, M. R.; Inganas, O. *Phys. Rev. B* **2000**, *61*, 12957.
(7) Markov, D. E.; Amsterdam, E.; Blom, P. W. M.; Sieval, A. B.; Hummelen, J. C. *J. Phys. Chem. A* **2005**, *109*, 5266.
(8) Rim, S.; Fink, R. F.; Schöneboom, J. C.; Erk, P.; Peumans, P. *Appl. Phys. Lett.* **2007**, *91*, 173504.
(9) Kenkre, V. M.; Parris, P. E.; Schmid, D. *Phys. Rev. B* **1985**, *32*, 4946.
(10) de la Torre, G.; Claessens, C. G.; Torres, T. *Chem. Commun.* **2007**, 2000.
(11) Gommans, H. H. P.; Cheyns, D.; Aernouts, T.; Girotto, C.; Poortmans, J.; Heremans, P. *Adv. Funct. Mater.* **2007**, *17*, 2653.
(12) Claessens, C. G.; González-Rodríguez, D.; Torres, T. *Chem. Rev.* **2002**, *102*, 835.
(13) González-Rodríguez, D.; Torres, T.; Guldi, D. M.; Rivera, J.; Ángeles, M.; Echegoyen, L. *J. Am. Chem. Soc.* **2004**, *126*, 6301.
(14) Mutolo, K. L.; Mayo, E. I.; Rand, B. P.; Forrest, S. R.; Thompson, M. E. *J. Am. Chem. Soc.* **2006**, *128*, 8108.
(15) Becker, H.; Burns, S. E.; Friend, R. H. *Phys. Rev. B* **1997**, *56*, 1893.
(16) del Rey, B.; Keller, U.; Torres, T.; Rojo, G.; Agullo-Lüpez, F.; Nonell, S.; Martí, C.; Brasselet, S.; Ledoux, I.; Zyss, J. *J. Am. Chem. Soc.* **1998**, *120*, 12808.
(17) Pope, M.; Swenberg, C. S. *Electronic Processes in Organic Crystals and Polymers*, 2nd ed.; Oxford University Press: New York, 1999; p 122.
(18) Chandrasekhar, S. *Rev. Mod. Phys.* **1943**, *15*, 1.
(19) Pettersson, L. A. A.; Roman, L. S.; Inganas, O. *J. Appl. Phys.* **1999**, *86*, 487.
(20) Gommans, H.; Verreet, B.; Rand, B.; Muller, P.; Poortmans, J.; Heremans, P.; Genoe, J. *Adv. Funct. Mater.*, **2008**, *18*, 3686–3691.

JP809802Q